Electronic Supplementary Material (ESI) for RSC Advances.

Supplementary information of:

Interface contact and modulated electronic properties by in-plain strains in graphene-MoS_2 heterostructure

Qian Wang[1], Zhenjun Song[2], Junhui Tao[1], Haiqin Jin[1], Sha Li[1], Yuran Wang[1], Yuejuan Liu[3], and Lin Zhang[1*]

[1]School of Physics and Mechanical & Electrical Engineering, Hubei Engineering Technology Research Center of Environmental Purification Materials, Hubei University of Education, Wuhan 430000, China,

[2] School of Parmaceutical and Materials Engineering, Taizhou University, Taizhou 318000, PR China

[3]College of Physics and Engineering, Chengdu Normal University, Chengdu 611130, China

* E-mail: zhanglin@hue.edu.cn

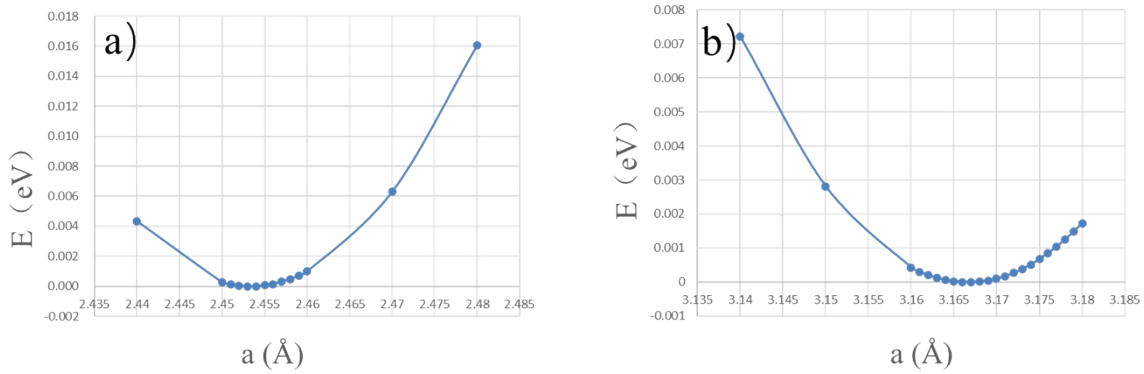

FIG. S1. Evolution of the total energy as a function of lattice parameter of (a) graphene and (b) MoS_2, taking the origin at the lowest energy configuration.

Fig. S1 shows the total energy curves of isolated graphene and MoS_2 monolayer. As shown, the lattice parameter of graphene and MoS_2 are 2.454 Å and 3.167Å.

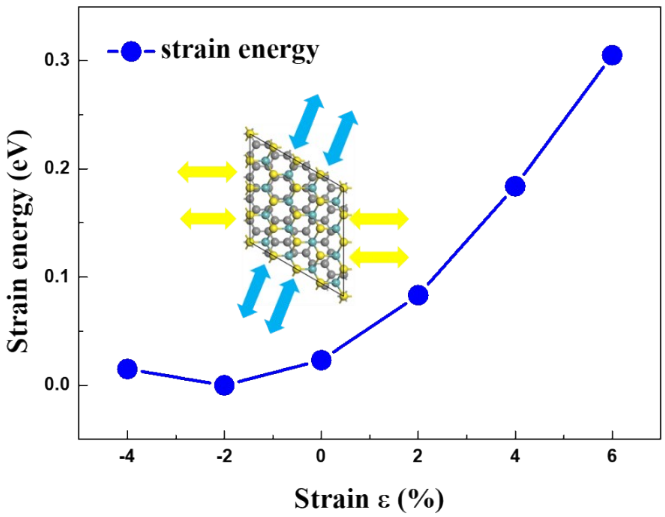

FIG. S2. The in-plane biaxial strain applied to Gr-MoS_2 heterojunction, and the relationship of strain energy with the biaxial strains.

The strain energy is checked here to ensure the strains considered are all within the elastic limit. The strain energy is given by the formula: $E = (E_S - E_U)/n$, where E_S and E_U are the total energy of strained and unstrained heterostructure, respectively, and n indicates the atom number in the supercell. Fig. S2 exhibits the relationship of the strain energy E with the imposed biaxial strain. In the biaxial strain range of -4% ~ 6%, it is obviously that the strain energy shows a characteristic of a quadratic function, which indicates that the mechanical strain falls within the elastic limit range that the deformed structure can restore to its initial state when the mechanical strains are removed.

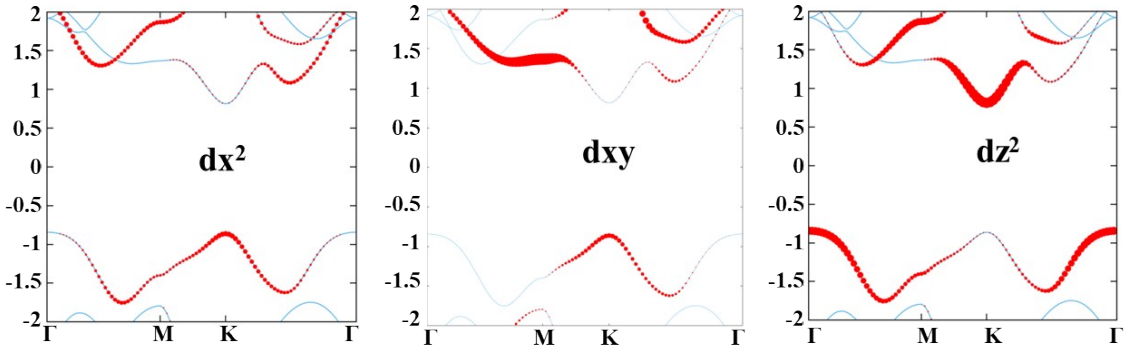

FIG. S3. The dx^2, dxy, dz^2 orbitals band structures of MoS_2.

Fig. S3 shows the dx^2, dxy, dz^2 orbitals band structures of MoS_2. It can be seen that the valence band minimum (VBM) of MoS_2 is located at the highly symmetric point K, which is contributed by the dz_2 orbital. Relatively, the conduction band maximum (CBM) is relatively complex, the CBM originates from the competition between the conduction band at K point contributed by dx^2 orbital, and the conduction band at Γ point contributed by dz^2 orbital. For MoS_2 monolayer with direct bandgap, CBM and VBM are both located at K.

While after adsorbed on graphene, the interaction in the direction perpendicular to the horizontal plane from graphene will enhance the MoS_2 dz^2 orbit, so that the CBM at Γ assumes a leading position and the direct bandgap in MoS_2 transforms to indirect.

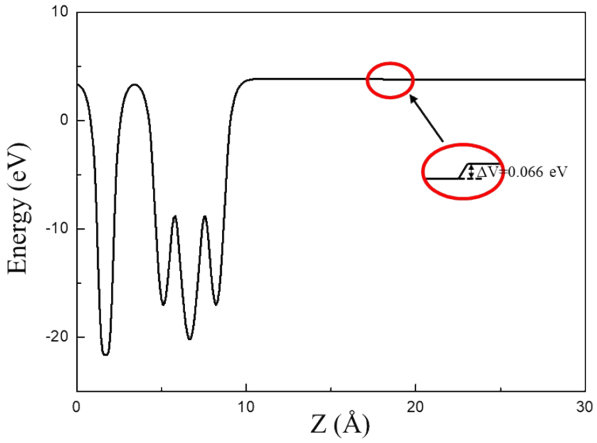

FIG. S4. The plane averaged electrostatic potentials of Gr-MoS_2 heterojunction along z-direction.

In Fig. S4, the average Coulomb potential for the Gr-MoS_2 system is shown. It can be seen that difference in work function in the case of Gr-MoS_2 and isolated graphene surface is defined as $\Delta V = W_{Gr-MoS2} - W_{Gr}$, and it is about 0.066 eV. As ΔV>0, electrons will be transferred from graphene to MoS_2 surface, making the n-type contact.

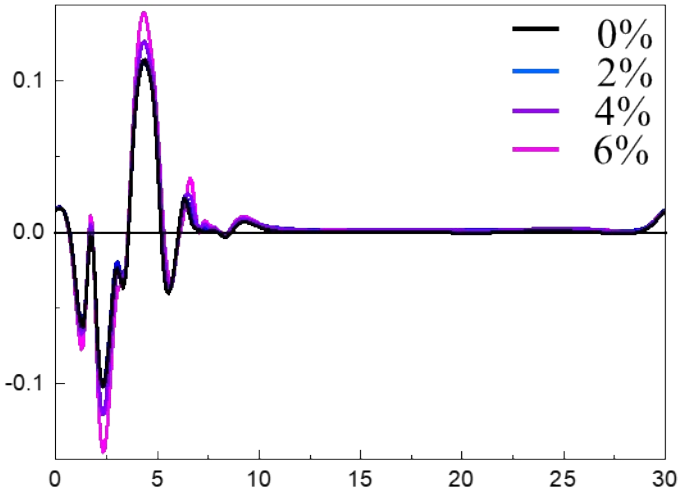

FIG. S5. Evolution of charge density differences under tensile strains.

Fig. S5 presents the charge density differences of Gr-MoS_2 bilayer under various in-plane tensile strains. It is clear that the electron redistribution mainly occurs within the strain. As mentioned, the electron accumulates and depletes on the side of MoS_2 and graphene layer, and it is observed that the degree of electron redistribution increases with increasing the strain, reaching a maximum value at 6%.

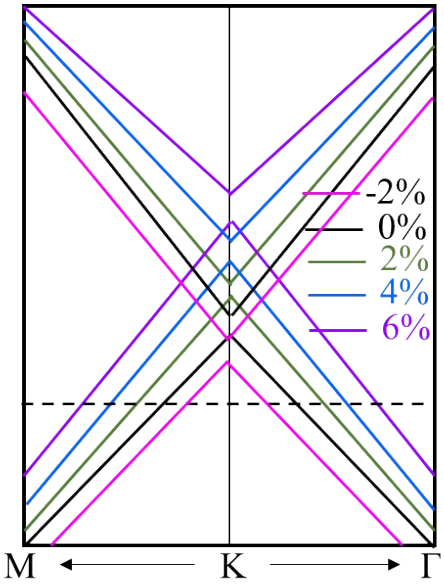

FIG. S6. Linear dispersion near the Fermi level at Dirac point of Gr-MoS_2 interface with tensile strain.

To describe the effect of the strain on the band gap of graphene in Gr-MoS_2 heterojunctions, in Fig. 6 we show the energy dispersion near the Fermi energy level at Dirac point for the VBM and the CBM in the band structures with different strain. As shown in Fig. S2, the total energy of Gr-MoS_2 junction is minimum at the equilibrium state of strain -2%, when graphene is subjected to the least external force. Therefore, for graphene, strain -2% is the most stable state. As mentioned above, the charge transfer from graphene to MoS_2, moves the Fermi level down below the Dirac point, leading to the hole doping in graphene in the Gr-MoS_2 heterojunction.

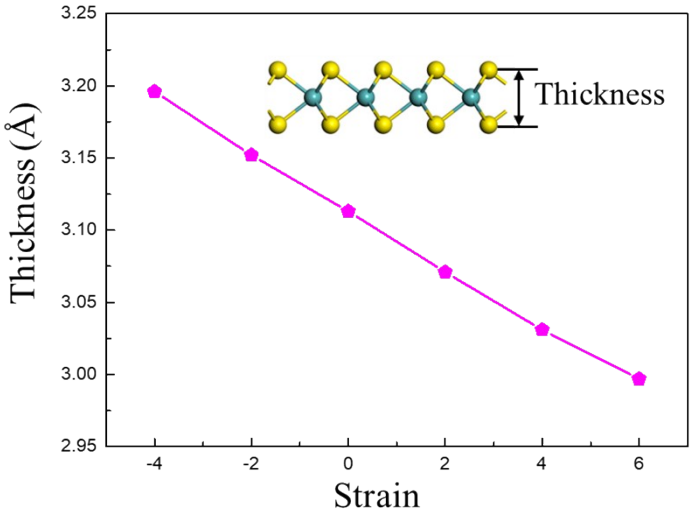

FIG. S7. The relationship of thickness of monolayer MoS_2 with the biaxial strains.

The thickness of layered MoS_2 changes with the application of strain, as shown in the Fig. S7. It can be seen that when compressive strain is applied, the thickness increases and Mo-S bond tends to the horizontal vertical direction, while when tensile strain is applied, its thickness decreases and Mo-S bond tends to the horizontal

direction. That is, the tensile strain in MoS_2 achieved by increasing lattice constant flattens the monolayer. Moreover, with tensile strain, the bond length of Mo-S is elongated, so that the ability of constraint valence electrons is weakened and then the band gap is reduced accordingly.